processes

MDPI

Article

Structural Changes of Alkali Lignin under Ozone Treatment and Effect of Ozone-Oxidized Alkali Lignin on Cellulose Digestibility

Hongyuan Wang, Lihong Zhao *, Junli Ren and Beihai He

State Key Laboratory of Pulp and Paper Engineering, South China University of Technology, Guangzhou 510000, China; liwanghy@mail.scut.edu.cn (H.W.); renjunli@scut.edu.cn (J.R.); ppebhhe@scut.edu.cn (B.H.)
* Correspondence: zhaolh@scut.edu.cn

Abstract: In this study, the structural changes of alkali lignin induced by ozonation were investigated, and the effect of ozone-treated alkali lignin and its mechanism on Avicel enzymatic hydrolysis was examined. The physicochemical properties of alkali lignin were analyzed by FTIR, ^{1}H-^{13}C HSQC NMR, and GPC. It was revealed that ozone pretreatment increased the content of carboxyl and/or aldehyde groups and the negative zeta potential of alkali lignin, which enhanced the electrostatic repulsion between alkali lignin and cellulase; The S/G ratio was reduced, indicating the hydrophobic interaction was diminished. The Langmuir adsorption isotherm showed that the cellulase binding strength of ozone pretreated alkali lignin (OL-pH3, OL-pH7, and OL-pH12 were 16.67, 13.87, and 44.05 mL/g, respectively) was significantly lower than that of alkali lignin (161.29 mL/g). The 72 h hydrolysis yields of Avicel added with OL-pH3, OL-pH7, and OL-pH12 were 55.4%, 58.6%, and 54.9% respectively, which were 2.6–6.3% higher than that of Avicel added with AL (52.3%). This research aimed to reduce the non-productive adsorption between cellulase and lignin by investigating the structural changes of lignin caused by ozone treatment. For the first time, we discovered that ozone-treated alkali lignin has a further promotion effect on the enzymatic digestion of cellulose, providing a green and feasible pretreatment process for the enzymatic hydrolysis of lignocellulose and aiding in the more efficient utilization of biomass.

Keywords: lignocellulose; alkali lignin; ozone treatment; enzymatic hydrolysis; cellulase; non-productive adsorption

check for updates

Citation: Wang, H.; Zhao, L.; Ren, J.; He, B. Structural Changes of Alkali Lignin under Ozone Treatment and Effect of Ozone-Oxidized Alkali Lignin on Cellulose Digestibility. *Processes* **2022**, *10*, 559. https://doi.org/10.3390/pr10030559

Academic Editors: Wei-Hsin Chen, Aristotle T. Ubando, Chih-Che Chueh and Liwen Jin

Received: 16 February 2022
Accepted: 11 March 2022
Published: 13 March 2022

Publisher's Note: MDPI stays neutral with regard to jurisdictional claims in published maps and institutional affiliations.

Copyright: © 2022 by the authors. Licensee MDPI, Basel, Switzerland. This article is an open access article distributed under the terms and conditions of the Creative Commons Attribution (CC BY) license (https://creativecommons.org/licenses/by/4.0/).

1. Introduction

In recent years, lignocellulose biomass has attracted increasing attention because of its advantages of low price, easy availability, and abundant reserves [1]. At the same time, numerous chemicals and material products continue to rely on a variety of non-renewable resources as raw materials, which runs counter to the social development trend toward sustainable development. The biorefinery of lignocellulose via enzymatic hydrolysis aims to convert cellulose and hemicellulose into monosaccharides and oligosaccharides, which can then be transformed into a variety of chemical products that are regarded as potential substitutes for plastics and fossil fuels, whose utilization would assist in alleviating the food issue [2]. However, the surfaces of carbohydrates are covered with lignin that exists in the lignocellulose cell wall, leading to a range of detrimental consequences on the enzymatic saccharification. Lignin is a polymer with a three-dimensional network structure formed by phenylpropane crosslinking units, which has amorphous rigidity and hydrophobicity [3,4], and whose obstinate structure acts as a major bottleneck for converting cellulose into glucose [5]. Lignin typically affects the enzymatic hydrolysis of lignocellulose in three ways: steric hindrance, comprising physical barriers generated by lignin wrapping around cellulose and hemicellulose surfaces and limiting cellulase accessibility to cellulose;

the induction of non-productive enzyme adsorption by ineffective lignin adsorption on cellulase, which can significantly lower enzymatic digestion efficiency; and the inhibition by lignin of cellulase activity [5–7].Thereinto, the non-productive adsorption of lignin with cellulase plays a leading role. As is well known, cellulase undergoes unproductive adsorption with lignin via hydrophobic, electrostatic, and hydrogen bonding interactions (primarily hydrophobic and electrostatic interactions), limiting the quantity of cellulase employed for cellulose hydrolysis, resulting in the waste of cellulase and raising the cost of enzymatic hydrolysis [8]. However, in recent years, it was found that the addition of lignin sulfonate is beneficial to the enzymatic efficiency under certain conditions, and it has an effect similar to that of an anionic surfactant. Moreover, it was reported that milled wood lignin, when treated by the Fenton reaction system, has a significant promotion effect on the enzymatic digestion of cellulose, which is contrary to our traditional view that lignin plays a negative role in the enzymatic system [9].

Biorefining is typically a three-step process that begins with pretreatment, followed by enzymatic hydrolysis and fermentation [10,11]. Pretreatment is the procedure that minimizes lignocellulose resistance especially derived from lignin and facilitates enzymatic saccharification [12]. Many studies on various pretreatment procedures have been conducted, including chemical approaches using strong acids, strong bases, and organic solvents such as ethanol, and physical methods using mechanical treatments such as ball milling [8]. Several of these chemical or physical pretreatment methods have been shown by previous researchers to be effective in reducing lignocellulose's biological resistance [13]; however, these chemical methods or coupled chemical–physical methods generate waste streams that are difficult to treat and have a negative impact on the natural environment. Furthermore, these procedures produce by-products such as numerous enzymatic and fermentation inhibitors, which not only lower the effectiveness of enzymatic digestion but are also harmful to the microbial culture of the fermentation [14].

Ozone is one of the most powerful oxidants and is highly reactive with compounds that have conjugated double bonds and functional groups with a high electron cloud density, such as the double bond and benzene ring in lignin [14,15]. It is reported that ozone treatment can effectively remove lignin of lignocellulose, enhance the accessibility of carbohydrates, and increase the yield of glucose [16–18]. Due to the difference in electronic properties between lignin and carbohydrate, ozone reacts with lignin at a rate 10^6 times that of carbohydrate. As a result, ozone can effectively remove lignin from lignocellulose while having little impact on cellulose, and the recovery of cellulose and hemicellulose can reach more than 90% [15,19,20]. Additionally, it has been reported that the removal rate of hemicellulose can be controlled by adjusting the amount of ozone used, and that removing hemicellulose increases the volume of lignocellulose micropores, further improving the accessibility of enzymatic hydrolysis and reducing the consumption of enzymes [21,22]. Fang et al. discovered that pretreatment with ozone and alkali may also alter the crystal structure of cellulose, increase the interlayer spacing, and make the crystalline form of cellulose more accessible to cellulase [23,24]. Furthermore, only by-products such as lactic acid, formic acid, xylitol, and acetic acid are formed during ozone treatment, which are readily eliminated with adequate water washing, and no inhibitors such as 5-hydroxyethyl furfural (HMF) and furfural are generated [14,19,25]. Numerous studies have been published on the effect of ozone treatment on the enzymatic digestibility of lignocellulose, but there is no detailed investigation into the molecular structural changes in lignin and non-productive adsorption of lignin with cellulase caused by ozone treatment, and the relationship with the efficiency of enzymatic hydrolysis. Therefore, the structural changes of alkali lignin under ozone treatment and the effect of ozone-oxidized alkali lignin on cellulose digestibility were investigated in this work. Typical alkali lignin extracted from the black liquor of chemical pulping in the paper industry was selected in this study. The functional groups of alkali lignin before and after ozone treatment were characterized by FTIR, GPC, and ^{1}H-^{13}C HSQC NMR, including condensed and non-condensed syringyl and guaiacyl hydroxyl, phenylcoumaran, resinol, and β-aryl ether bond. Alkali lignin

was treated with ozone at a range of pH values (3–12) and yielded three distinct ozone-treated alkali lignins (OL-pH3, OL-pH7, OL-pH12). The Langmuir adsorption isotherm was utilized to assess the affinity of alkali lignin for the cellulase. Additionally, alkali lignin's zeta potential and hydrophobicity were also determined. The purpose of this work was to clarify the effects of ozone treatment on the molecular structure of alkali lignin and its adsorption to cellulase, and to elaborate the effect of ozone-treated alkaline lignin on cellulose digestion by discussing the connection between the structural changes and its adsorption with cellulase of alkali lignin.

2. Materials and Methods

2.1. Materials

Alkali lignin was extracted from hardwood pulping black liquor, provided by Hunan Juntai New Material Technology Co., Ltd., and purified by an acidulation precipitation method. Alkali lignin is composed of 91.5% acid-insoluble lignin, 3.27% acid-soluble lignin, 0.1% glucan, 0.06% xylan, 2.55% ash, and 2.52% others (based on dry weight). Ctec-3 with the filter paper activity of 215 FPU/mL and the β-glucosidase activity of 51 CBU/mL was utilized in the following enzymatic hydrolysis experiment of cellulose. Cellulast 1.5 L from Sigma-Aldrich with the filter paper activity of 81 FPU/mL was used for the cellulase adsorption experiment. The microcrystalline cellulose employed for enzymatic hydrolysis experiment was pharmaceutical grade (AvicelPH-101, Sigma-Aldrich, Shanghai, China.

2.2. Purification of Alkali Lignin

Alkaline lignin was dissolved in NaOH (10%) solution, heated, and stirred for 2 h at 90 °C by a magnetic stirrer, and then insoluble impurities were removed by suction filtration after complete dissolution. The pH value was adjusted to 2 by hydrochloric acid. The static solution was stratified until the supernatant was clarified. Finally, alkali lignin was purified by suction filtration, washing, and drying in sequence.

2.3. Pretreatment of Alkali Lignin by Ozone

The reactor of the self-designed ozone generator unit was loaded with alkaline lignin with a solid content of 3% and the solution was adjusted to pH3, pH7, and pH12. Then, alkali lignin was ozone treated with an ozone concentration of 85 mg/L and a flow rate of 3 L/min for 45 min. Ozone was produced using an ozone generator (CF-G-3-10g, Guolin, Qingdao, China) and industrial grade (99.5%) oxygen. The ozone concentration at the entrance of the reactor was monitored with a concentration detector. Following the treatment, the ozone treated lignin was cleaned with deionized water and vacuum filtered to eliminate possible inhibitors, and then the product was vacuum dried. Original alkali lignin and lignins obtained by ozone treatment at pH3, pH7, and pH12 are named AL, OL-pH3, OL-pH7, and OL-pH12, respectively.

2.4. Enzymatic Hydrolysis of Avicel with Lignin Samples

Under the condition of Avicel concentration of 2% (*w/v*) and enzyme load of 20 FPU/g, enzymatic hydrolysis was carried out at 50 °C, 150 rpm, and pH 4.8 for 72 h. To evaluate the influence of alkali lignin on enzymatic hydrolysis, four lignin samples (AL, OL-pH3, OL-pH7, OL-pH12) (10 g/L) were added to the enzymatic hydrolysis experiment of Avicel, respectively. At 4, 8, 12, 24, 48, 72 h during the enzymatic hydrolysis process, 1 mL of the supernatant was sampled to determine the sugar release and the quantity of free cellulase. The sugar release was evaluated using HPLC after the supernatant went through a 0.22 μm water filter membrane. The protein content of the supernatant was measured by bicinchoninic acid (BCA) assay, with BSA serving as the standard.

2.5. Cellulase Adsorption Isotherm on Alkali Lignin

To examine the adsorption isotherm of cellulase on lignin in biomass, cellulase (0.01–1.0 mg/L) and alkali lignin (5 g/L) were incubated in 50 mM citrate buffer solu-

tion (pH4.8) at 4 °C and 150 rpm for 3 h. After the incubation reached equilibrium, the adsorption mixture was centrifuged at 10,000 rpm for 5 min, and the supernatant was collected for protein content measurement. The quantity of cellulase adsorbed was determined by comparing the original enzyme concentration to the free enzyme concentration in the supernatant. The adsorption of cellulase on alkali lignin was characterized by the Langmuir adsorption isotherm. The formula [26] is as follows:

$$\frac{1}{\Gamma} = \frac{1}{K \cdot [\Gamma_{max}] \cdot C} + \frac{1}{\Gamma_{max}}$$

where C is the concentration of free protein in the solution (mg/mL), Γ is the concentration of enzyme adsorbed on lignin surface (mg/mL), and Γ_{max} is the concentration of protein when the lignin surface is completely covered with enzyme (mg/mL), describing the theoretical maximum adsorption capacity of lignin to the enzyme. K is the Langmuir constant (mL/mg), which represents the lignin–enzyme adsorption affinity. K and Γ_{max} are obtained by linear fitting of the experimental data according to the adsorption isotherm. R denotes the binding strength of lignin to the enzyme, as determined by K and Γ_{max} ($R = K \cdot \Gamma_{max}$).

2.6. Characterization of Alkali Ligni

Rose Bengal dye was used to measure the hydrophobicity of alkali lignin. The lignin was dispersed in Rose Bengal solution (40 mg/L, pH4.8) in a gradient lignin concentration range of 2–10 g/L, and incubated at 50 °C under shaking (150 rpm) for 2 h. The absorbance of free Rose Bengal dye in the supernatant was measured with a UV–vis spectrophotometer at the wavelength of 543 nm. The concentration of free dye in the supernatant was calculated through the standard curve of dye concentration and absorbance relationship. The partition coefficient (PQ) is the ratio of adsorbed dye concentration to free dye concentration, which is linearly related to lignin content, and the slope of the line is used to characterize the hydrophobicity (L/g) of the sample.

Lignin samples were disseminated in 50 mM citric acid buffer at a concentration of 0.1% (*w/v*) and oscillated in a shaking table at 50 °C and 150 rpm for 1 h. Three measurements of the zeta potential were averaged.

2.7. Analytical Methods

The surface morphology of alkali lignin before and after ozone treatment was observed by scanning electron microscopy (EVO 18, Zeiss, Germany). Before testing, the lignin attached to the conductive adhesive was coated with Au.

The distribution of various elements in the alkali lignin samples was analyzed by elemental analyzer (Vario EL, Elementar, Germany), where the oxygen content was obtained by the differential subtraction method [27].

The weight average molecular weight (M_w) and number average molecular weight (M_n) of samples were determined by gel permeation chromatography (GPC). The pretreated lignin was derivatized using an acetic anhydride/pyridine (1:2, *v/v*) combination at room temperature for 24 h. The derivatized samples were dissolved in tetrahydrofuran for GPC analysis. The molecular weight was estimated by size-exclusion separation on an Agilent 1200 high-performance liquid chromatography system.

Fourier Transform Infrared Spectroscopy was used to examine the infrared spectra of alkali lignin. The detection conditions were as follows: both the sample and K/Br were dried at 105 °C for 4 h to absolute dryness. Under the irradiation of the infrared lamp, the dried sample was mixed with K/Br in the mass ratio of 1:100. The samples were scanned 64 times at a wavelength of 4000–500 cm^{-1} and a resolution of 2 cm^{-1}.

^{1}H-^{13}C HSQC NMR spectra of alkali lignin were collected by a nuclear magnetic resonance instrument (500 HZ, Brooke, Germany) at 20 °C. A sample of 100 mg lignin was weighed and dissolved in 1000 μL DMSO-d6. ^{1}H-^{13}C HSQC chemical shift correction was carried out based on the DMSO solvent peak position.

3. Results and Discussion

3.1. SEM Microscopy

The surface morphology of alkali lignin before and after ozone treatment is shown in Figure 1. The surface of untreated alkali lignin was generally smooth and flat, although some lignin debris existed. However, after ozone treatment, the surface became defective; in particular, holes and cracks appeared in OL-pH3, and roughness and wrinkles increased, indicating that the strong oxidation of ozone also slightly damaged the physical structure of lignin.

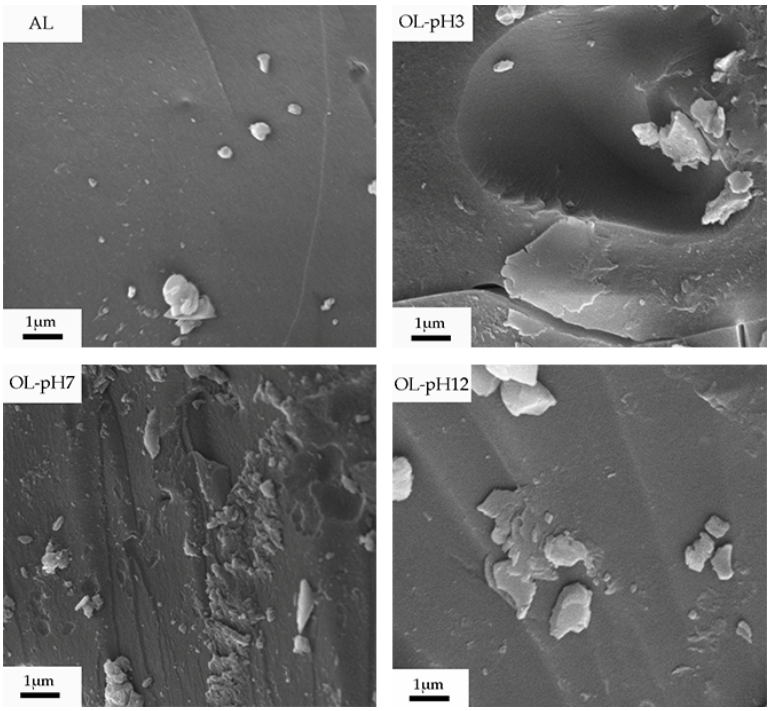


Figure 1. Scanning electron microscopy (SEM) images of alkali lignin before and after ozone pretreatments.

3.2. Elemental Analysis

The carbon, hydrogen, and oxygen contents of alkali lignin were measured by elemental analysis, and the C_{900} formula and the degree of unsaturation were evaluated [28], as shown in Table 1. After ozone treatment, the carbon and hydrogen contents of alkali lignin increased, whereas the oxygen content decreased, and the unsaturation degree of all alkali lignins increased. This indicates that alkali lignin contains more unsaturated bonds after ozone treatment, such as unsaturated double bonds in the side chain of aromatic rings.

Table 1. Elemental content and degree of unsaturation of alkali lignin before and after ozone pretreatments.

Samples	C (%)	H (%)	O (%)	C_{900} Formula	Degree of Unsaturation
AL	58.41	5.51	34.39	$C_{900}H_{1019}O_{397}$	391
OL-pH3	61.65	5.59	31.76	$C_{900}H_{979}O_{348}$	411
OL-pH7	61.63	5.52	31.97	$C_{900}H_{967}O_{350}$	417
OL-pH12	64.15	5.74	29.07	$C_{900}H_{966}O_{306}$	418

3.3. Fourier Transform Infrared Spectrum (FTIR) Analysis

Figure 2 illustrates the infrared spectra of components for the four lignins. As shown in Table 2, the relative signal intensity of each functional group was calculated with reference to the intensity in the 1514 cm^{-1} band. The peaks at 1608, 1514, and 1426 cm^{-1} correspond to the tensile vibration of the lignin aromatic ring skeleton, which are the characteristic absorptions of lignin [24,29]. No significant change was monitored, indicating

that the main structure of lignin remained unchanged following ozone treatment. Weaker peaks corresponding to the C-H bonds of the methoxy and methyl, assigned to 2937 and 2840 cm^{-1}, were observed in the pretreated lignin. This change could be attributed to the degradation of AL by the pretreatment [20]. The peaks at 1325 and 1113 cm^{-1} represent the C-O vibration on the syringyl-based aromatic ring and C-H deformation inside the aromatic ring [23,30]. The peaks for the C=O tensile vibration and C-O vibration signals on the guaiacyl ring were assigned to 1269 and 1214 cm^{-1} [30]. The infrared spectrum reveals that the signal intensity of the four lignin samples varied, implying that the S/G ratio of alkali lignin was altered following ozone treatment. The strong band at 3452 cm^{-1} is attributed to the stretching vibration of the hydroxyl group in lignin, which includes both aliphatic and aromatic hydroxyl. The peak intensity of the hydroxyl group showed an increase with the ozone treatment. These could be primarily due to the breaking of the ether bond and the formation of additional hydroxyl groups during the ozone treatment. An increase in ozone pretreated lignin was observed at 1703 cm^{-1}, which represents tensile vibration signals of C=O [24,31]. This change may be due to the oxidation of α-OH or γ-OH in the alkali lignin, demonstrating that the modification of lignin by ozone results in the formation of more nonconjugated carbonyl compounds, and suggesting that a large number of aldehyde groups and/or carboxyl groups are likely to be introduced during ozone modification, which is consistent with the results of previous studies [23].

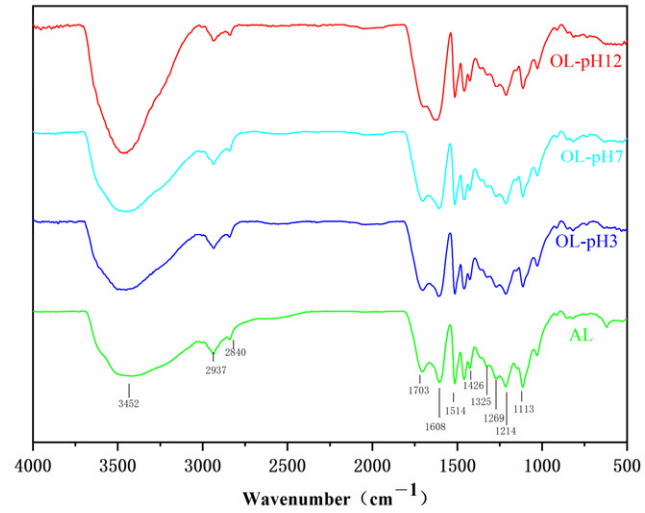


Figure 2. FTIR spectra of alkali lignin before and after ozone pretreatments.

Table 2. The relative signal intensity of each functional group based on the 1514 cm^{-1} band.

Assignment	Wavenumber cm^{-1}	AL	OL-pH3	OL-pH7	OL-pH12
Hydroxyl group	3452	0.88	0.95	1.09	1.76
C-H stretching	2937	0.57	0.38	0.46	0.22
methoxy C-H	2840	0.39	0.23	0.27	0.15
carbonyl group	1703	0.82	0.95	0.95	1.13
Aromatic ring	1608	0.98	1.03	1.05	1.31
Aromatic ring	1514	1.00	1.00	1.00	1.00
C-H deformation	1460	0.91	0.93	0.93	0.91
Aromatic ring	1426	0.77	0.80	0.81	0.77
C-O vibration of syringyl	1325	0.75	0.77	0.76	0.68
Guaiacyl C-O units	1269	0.92	0.91	0.89	0.85
C-O vibration of guaiacyl	1214	1.04	1.00	0.98	0.97
Aromatic C-H deformation in syringyl	1113	1.04	0.90	0.89	0.88
C-O-C stretching	1029	0.60	0.62	0.61	0.60
Aromatic C-H deformation out of plane	815	0.10	0.13	0.14	0.17

3.4. ^{1}H-^{13}C HSQC NMR Spectral Analysis

The structural information of alkali lignin was obtained by HSQC NMR. Its 2D HSQC spectrum is shown in Figure 3. The aromatic region (100–135/6.0–8.0 ppm) of HSQC spectrum is dominated by guaiacyl (G) (C_2/H_2, δ_C/δ_H 110.5/6.89) (C_5/H_5, δ_C/δ_H 115.2/6.96) (C_6/H_6, δ_C/δ_H 119.0/6.82), α-oxidized syringyl (S′) ($C_{2,6}/H_{2,6}$, δ_C/δ_H 106.3/7.29), syringyl (S) ($C_{2,6}/H_{2,6}$, δ_C/δ_H 103.6/6.68). The aromatic components of hardwood alkali lignin are composed of S and G units, each of which can be measured by using volume integration [29,32,33]. Table 3 summarizes the semi-quantitative information of lignin subunits and linkages in the HSQC NMR of each lignin sample. After ozone treatment, the correlation signal of syringyl unit was reduced, while the signal of guaiacyl unit remained strong. This may be due to the loss of a methoxy group from the syringyl unit and its conversion to the guaiacyl unit, resulting in a drop in the S/G ratio of alkali lignin from 0.64 (AL) to 0.52 (OL-pH3), 0.55 (OL-pH7), and 0.52 (OL-pH12). In the aliphatic region (50–90/2.5–5.5 ppm) of the HSQC NMR spectrum, the most notable signal identified in all spectra was β-O-4 aryl ether (A). The C–H correlations of A_γ (C_γ-H_γ in β-O-4) and C_γ (C_γ-H_γ in phenylcoumaran (β-5)) were observed in alkali lignin at δ_C/δ_H 59.6/3.58 and δ_C/δ_H 63.1/3.52 ppm, respectively. Additionally, the cross peak for B_α (C_α-H_α in resinol (β-β)) and B_γ (C_γ-H_γ in resinol (β-β)) was present in alkali lignin at δ_C/δ_H 85.1/4.6 and δ_C/δ_H 71.5/3.80–4.13 ppm, respectively. These results suggest that β-O-4 aryl ether is the main inter-unit linkage of alkali lignin, accounting for nearly 93.1% of the total linkages, followed by β-β (5.3%) and β-5 (1.6%). Through ozone treatment under the neutral condition (OL-pH7), the contents of the β-O-4 aryl ether decreased to 71.4%; thus, it is possible that the β-O-4 aryl ether is easier to shear under neutral conditions. In addition, the contents of β-5 in OL-pH7 (<0.1%) and OL-pH12 (<0.1%) were relatively lower than those in AL (1.6%). It was revealed that ozone pretreatment would result in more breaks in β-5 than in β-O-4 and β-β under neutral and alkaline conditions.

Table 3. Semi-quantitative information for lignin subunits and inter-unit linkages in the untreated and ozone pretreated alkali lignin.

Lignin Substructure	AL		OL-pH3		OL-pH7		OL-pH12	
	% [a]	% [b]	% [a]	% [b]	% [a]	% [b]	% [a]	% [b]
S	40.0		34.2		35.5		34.2	
G	60.0		65.8		64.5		65.8	
S/G	0.64		0.52		0.55		0.52	
β-O-4	27.9	93.1	31.6	80.6	8.6	71.4	31.1	93.6
β-β	1.6	5.3	7.0	17.7	3.5	28.6	2.1	6.4
B-5	0.5	1.6	0.7	1.7	<0.1	<0.1	<0.1	<0.1

[a] Quantity of the specific functional group is expressed as a percentage of S + G. [b] Quantity of the specific functional group is expressed as a fraction of β-O-4 + β-5 + β-β.

3.5. Gel Permeation Chromatography (GPC) Analysis

The findings of the number average molecular weight (M_n), weight average molecular weight (M_w), and polydispersity (PDI) of different lignin samples are summarized in Table 4. The results demonstrate that ozone treatment reduced the number average molecular weight (M_n) and weight average molecular weight (M_w) of alkali lignin, indicating alkali lignin was degraded through ozone pretreatment, which was in accordance with the infrared spectra results. AL had a weight average molecular weight (M_w) of 14,116 g/mol, whereas the M_w of ozone-treated alkali lignin decreased to 10,667 g/mol (OL-pH3), 12,474 g/mol (OL-pH7), and 13,192 g/mol (OL-pH12). Previous studies confirmed that the depolymerization and recondensation of lignin typically occur concurrently during the chemical pretreatment process. It was proposed that the breaking of the ether bond in the initial stage of the ozone reaction reduces the molecular weight of alkali lignin, and fragmented lignin also condenses. However, with the extension of reaction time, the condensation reaction reversed the drop in the AL molecular weight, resulting in only a

slight decrease in the molecular weight of AL [34,35]. The polydispersity (PDI) of both AL and the three OLs was low (<2.4), which indicated that the molecular weight distribution of lignin components was narrow [36].

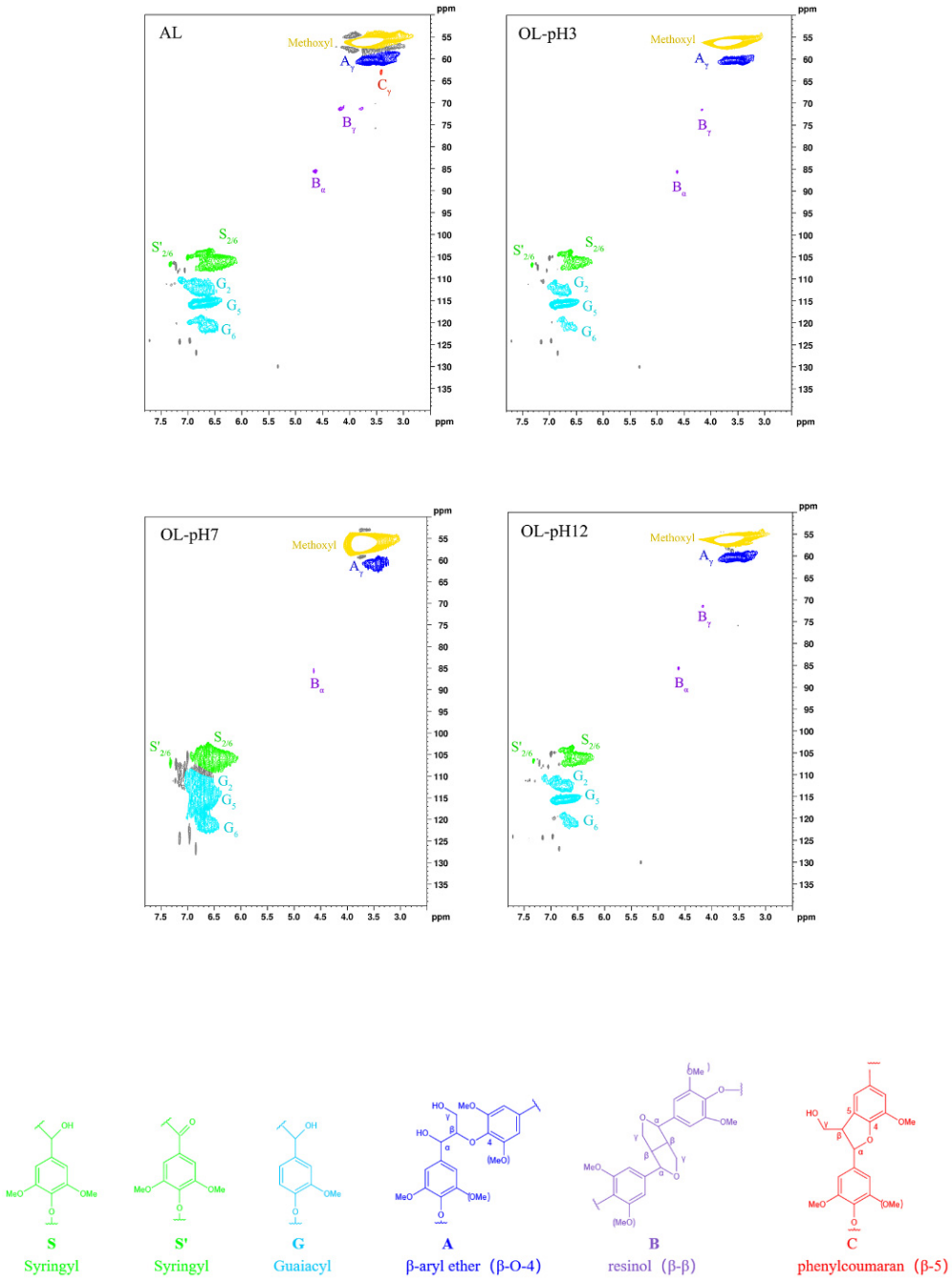


Figure 3. ^{1}H-^{13}C HSQC NMR spectra from the untreated and ozone pretreated alkali lignin.

Table 4. Weight average (M_w) and number average (M_n) molecular weights, and polydispersity indexes (M_w/M_n), of the four lignin samples.

Samples	M_n (g/mol)	M_w (g/mol)	PDI
AL	7146	14,116	1.98
OL-pH3	5154	10,667	2.07
OL-pH7	5384	12,474	2.32
OL-pH12	5946	13,192	2.22

3.6. Surface Properties of Lignin Preparations

Hydrophobic interaction as the main feature of non-productive adsorption of cellulase to lignin was characterized by the Rose Bengal method, which was used to measure the hydrophobicity of the surface of the lignins. As shown in Table 5, the hydrophobicity of AL was 0.137 L/g, whereas the hydrophobicity of OL-pH3, OL-pH7, and OL-pH12 was 0.040, 0.043, and 0.073 L/g, respectively. Compared with AL, the hydrophobicity of OL decreased by 46.7–70.8%. The reason why these three OLs have strong relative hydrophilicity may be related to the decrease in the S/G ratio, which is consistent with the analysis results of HSQC NMR [8,9,33,37]. It may also be due to the introduction of hydrophilic groups, such as ketone and carboxyl groups; as shown in the FTIR spectrum, the signal intensity at 1703 cm^{-1} of OLs is greater than that of AL [9,37].

Table 5. The physicochemical properties of untreated and ozone pretreated alkali lignin.

Samples	Zeta Potential (mV)	Hydrophobicity (L/g)
AL	−7.3	0.137
OL-pH3	−23.9	0.040
OL-pH7	−25.7	0.043
OL-pH12	−17.1	0.073

The charge properties of lignin were regarded as another important physicochemical feature. As shown in Table 5, the zeta potential of ozone-treated alkali lignin (OL-pH3, OL-pH7, and OL-pH12) decreased to −23.9, −25.7, and −17.1 mV respectively; compared with AL (−7.3 mV), the negative zeta potential increased by 2.27, 2.52, and 1.34 times. The higher negative zeta potential of OLs will produce stronger electrostatic repulsion between cellulase and negatively charged protein [38,39]. Therefore, less non-productive adsorption of cellulase on lignin will be achieved due to the stronger electrostatic repulsion.

3.7. Effects of Alkaline Lignin Modification on Nonproductive Adsorption of Cellulase

The Langmuir adsorption isotherm of cellulase on lignin samples was studied to investigate the effect of ozone treatment on the interaction between cellulase and lignin, and the maximum adsorption capacity, affinity, and binding strength were estimated, as shown in Table 6. The maximum adsorption capacity (Γ_{max}) of AL to cellulase was 27.55 mg/g, whereas the Γ_{max} of the OLs decreased to 25.91, 14.49, and 12.84 mg/g, respectively (OL-pH3, OL-pH7, and OL-pH12). The reason for this phenomenon may be that there are fewer binding sites on the surface of the OLs, which could be caused by the interruption of functional groups (such as phenolic hydroxyl groups) and branches of alkali lignin during ozone pretreatment [5]. The affinity (K value) of AL to cellulase is 5.86 mL/mg. After ozone treatment, the affinity of three OL samples to cellulase was significantly reduced, to 0.64, 0.96, and 3.43 mL/mg (OL-pH3, OL-pH7, and OL-pH12), respectively, and showed a decrease of 56.3–89.3%. In addition, the partition coefficient (R) is typically used to estimate the binding strength between cellulase and substrate. AL has a relatively high binding strength (161.29 mL/g), whereas the binding strength of OLs to cellulase was remarkably lower than that of AL, and was 16.67 mL/g (OL-pH3), 13.87 mL/g (OL-pH7), and 44.05 mL/g (OL-pH12). Therefore, there is less non-productive adsorption between OL samples and cellulase, which is possibly correlated to weak hydrophobicity and the high surface negative charge resulting from ozone pretreatment. In other words, both hydrophobic interaction and electrostatic interaction collectively reduce the non-productive adsorption of cellulase on alkali lignin.

Table 6. Langmuir adsorption isotherm parameters of enzyme adsorption on alkali lignin.

Substrates	Γ_{max} (g/g)	K (mL/mg)	R (mL/g)	R^2
Avicel	39.06	8.26	322.58	0.978
AL	27.55	5.86	161.29	0.972
OL-pH3	25.91	0.64	16.67	0.991
OL-pH7	14.49	0.96	13.87	0.986
OL-pH12	12.84	3.43	44.05	0.935

3.8. Effects of Alkaline Lignin Modification on Glucose Yield and Cellulase Distribution in Enzymatic Saccharification of Avicel

The enzymatic hydrolysis and saccharification of Avicel was investigated in the presence of pretreated alkali lignin. It is well known that lignin is usually an inhibitor of enzymatic hydrolysis and saccharification. Through hydrophobic, electrostatic, hydrogen bonding interactions, and non-productive adsorption, the enzymatic hydrolysis efficiency is usually negatively affected [40]. Interestingly, in this study, the addition of AL and OLs not only has no inhibitory effect on enzymatic hydrolysis, but also had a slightly positive effect. As shown in Figure 4, all four kinds of alkali lignin slightly promoted the enzymatic hydrolysis of Avicel. The addition of AL increased the 72 h glucose yield of Avicel from 48.3% to 52.3%. Moreover, after adding ozone-treated alkali lignins (OL-pH3, OL-pH7, and OL-pH12), the glucan digestibility of Avicel was further increased to 55.4%, 58.6%, and 54.9% respectively. In particular, after mixing OL-pH7 (10 g/L) with Avicel, the enzymatic hydrolysis efficiency of Avicel was increased by 6.3% compared with the mixing of AL and Avicel. In addition, the effect of cellulase distribution on the enzymatic hydrolysis process was investigated by analyzing the content of free enzymes in supernatant during the enzymatic hydrolysis process. It has been reported that there is a high association between the glucan digestibility of Avicel and the concentration of free cellulase in the adsorption process [9,41,42]. As shown in Figure 4, when Avicel was hydrolyzed alone, the protein content was 73.8% at 4 h and 85.4% at 72 h. The addition of AL and OLs increased the free enzyme concentration in the solution to 74.6% (AL), 77.6% (OL-pH3), 75.8% (OL-pH7), and 79.9% (OL-pH12) at 4 h. At 72 h, they increased to 93.3% (AL), 94.4% (OL-pH3), 95.3% (OL-pH7), and 94.9% (OL-pH12). These results show that the addition of AL improved the efficiency of enzymatic hydrolysis, most likely due to the competitive adsorption of AL and Avicel. However, as shown in Table 6, the affinity and the binding strength of alkali lignin for adsorption were less than those of Avicel. As a result, the cellulase was more easily desorbed off the lignin surface and the amount of free enzyme in the system was even greater than when Avicel alone was digested; thus, the efficiency of enzymatic hydrolysis was improved from 48.3% to 52.3%. Moreover, compared with AL, the addition of OLs, especially OL-pH7, further increased the content of free enzymes involved in enzymatic hydrolysis in the solution and significantly increased the glucose yield. According to the results shown in Tables 5 and 6, this may be caused by the reduction in the non-productive adsorption of lignin on cellulase after ozone treatment, which promoted the enzymatic hydrolysis and saccharification of Avicel. Many previous studies have reported improving the glucose yield of Avicel by reducing the unproductive adsorption between cellulase and lignin. Wu et al. found that the glucose yield of Avicel increased by 12.0–17.4% when the MWL treated by the Fenton system was added compared with mixing MWL. This was mainly due to the decrease in the proportion of syringyl and guaiacyl units in lignin and the increase in the negative zeta potential [9], inwhich the molecular structural changes in lignin were similar to the results of the ozone treatment in this study.

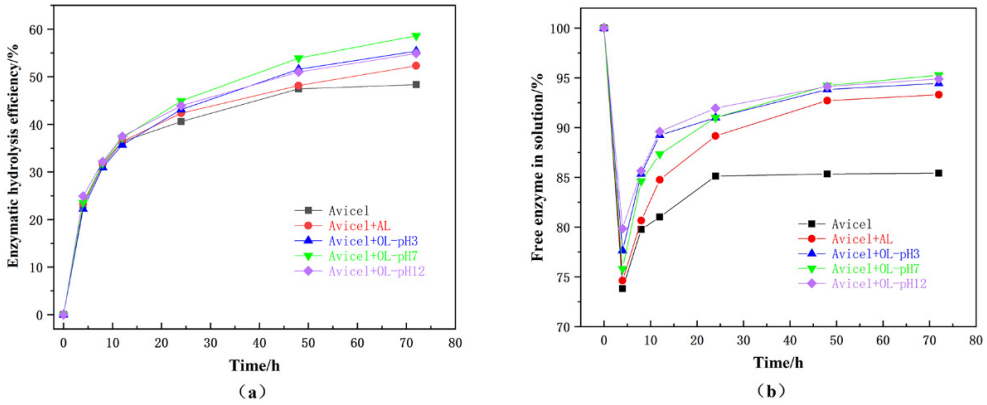


Figure 4. Effects of untreated and ozone pretreated alkali lignin on enzymatic hydrolysis efficiency (**a**) and cellulase distribution (**b**) in enzymatic hydrolysis of Avicel.

4. Conclusions

The presence of lignin in lignocellulose greatly limits the accessibility and chemical conversion of cellulose, so it is critical to find a suitable pretreatment to remove and/or modify lignin from lignocellulose. In this work, the effects of ozone treatment on the physical structures and chemical properties of alkali lignin and its adsorption properties with cellulase were investigated. This study revealed ozone treatment increased the contents of aldehyde and/or carboxyl groups and the negative zeta potential of alkali lignin, and enhanced the electrostatic repulsion between lignin and cellulase, whereas the decrease in the S/G ratio weakened the hydrophobic interaction. The Langmuir adsorption isotherm suggested that the maximum adsorption capacity, adsorption affinity, and binding strength of ozone-treated alkali lignin with cellulase were much lower than those of untreated alkali lignin. The addition of ozone-treated alkali lignin increased the glucan digestibility of Avicel from 52.3% (AL) to 58.6% (OL-pH7). In this study, ozone pretreatment was performed only for alkaline lignin, and further studies can be conducted for more species of lignin, such as milled wood lignin, cellulolytic enzyme lignin, and sulfonated lignin. Nevertheless, the investigation in this work of the effect on the structure and physicochemical properties of lignin, in addition to its non-productive adsorption with cellulase under ozone pretreatment, is conducive to developing appropriate pretreatment processes. These processes can ameliorate the effect of lignin during enzymatic digestion by reducing the non-productive adsorption of cellulase on lignin, and promote the efficient and comprehensive utilization of lignocellulose in the field of enzymatic hydrolysis.

Author Contributions: Conceptualization, H.W. and L.Z.; methodology, H.W.; software, H.W.; validation, H.W. and L.Z.; formal analysis, H.W.; investigation, H.W.; resources, L.Z., J.R. and B.H.; data curation, H.W.; writing—original draft preparation, H.W.; writing—review and editing, L.Z.; visualization, H.W.; supervision, L.Z.; project administration, L.Z., J.R. and B.H.; funding acquisition, L.Z., J.R. and B.H.; All authors have read and agreed to the published version of the manuscript.

Funding: This work was supported by the Key Area R&D Program of Guangdong Province (2020B0101070001).

Institutional Review Board Statement: Not available.

Informed Consent Statement: Not available.

Data Availability Statement: Not available.

Conflicts of Interest: The authors declare no conflict of interest. The funders had no role in the design of the study; in the collection, analyses, or interpretation of data; in the writing of the manuscript, or in the decision to publish the results.

References

1. Akhade, S.A.; Singh, N.; Gutierrez, O.Y.; Lopez-Ruiz, J.; Wang, H.; Holladay, J.D.; Liu, Y.; Karkamkar, A.; Weber, R.S.; Padmaperuma, A.B.; et al. Electrocatalytic Hydrogenation of Biomass-Derived Organics: A Review. *Chem. Rev.* **2020**, *120*, 11370–11419. [CrossRef]
2. Rahikainen, J.L.; Martin-Sampedro, R.; Heikkinen, H.; Rovio, S.; Marjamaa, K.; Tamminen, T.; Rojas, O.J.; Kruus, K. Inhibitory effect of lignin during cellulose bioconversion: The effect of lignin chemistry on non-productive enzyme adsorption. *Bioresour Technol.* **2013**, *133*, 270–278. [CrossRef] [PubMed]
3. Saini, J.K.; Patel, A.K.; Adsul, M.; Singhania, R.R. Cellulase adsorption on lignin: A roadblock for economic hydrolysis of biomass. *Renew. Energy* **2016**, *98*, 29–42. [CrossRef]
4. Szalaty, T.J.; Klapiszewski, Ł.; Jesionowski, T. Recent developments in modification of lignin using ionic liquids for the fabrication of advanced materials–A review. *J. Mol. Liq.* **2020**, *301*, 112417. [CrossRef]
5. Huang, C.; He, J.; Min, D.; Lai, C.; Yong, Q. Understanding the Nonproductive Enzyme Adsorption and Physicochemical Properties of Residual Lignins in Moso Bamboo Pretreated with Sulfuric Acid and Kraft Pulping. *Appl. Biochem. Biotechnol.* **2016**, *180*, 1508–1523. [CrossRef] [PubMed]
6. Yarbrough, J.M.; Mittal, A.; Mansfield, E.; Taylor, L.E., 2nd; Hobdey, S.E.; Sammond, D.W.; Bomble, Y.J.; Crowley, M.F.; Decker, S.R.; Himmel, M.E.; et al. New perspective on glycoside hydrolase binding to lignin from pretreated corn stover. *Biotechnol. Biofuels* **2015**, *8*, 214. [CrossRef] [PubMed]
7. Zhao, X.; Meng, X.; Ragauskas, A.J.; Lai, C.; Ling, Z.; Huang, C.; Yong, Q. Unlocking the secret of lignin-enzyme interactions: Recent advances in developing state-of-the-art analytical techniques. *Biotechnol. Adv.* **2021**, *54*, 107830. [CrossRef]
8. Yoo, C.G.; Li, M.; Meng, X.; Pu, Y.; Ragauskas, A.J. Effects of organosolv and ammonia pretreatments on lignin properties and its inhibition for enzymatic hydrolysis. *Green Chem.* **2017**, *19*, 2006–2016. [CrossRef]
9. Wu, K.; Ying, W.; Shi, Z.; Yang, H.; Zheng, Z.; Zhang, J.; Yang, J. Fenton reaction-oxidized bamboo lignin surface and structural modification to reduce nonproductive cellulase binding and improve enzyme digestion of cellulose. *ACS Sustain. Chem. Eng.* **2018**, *6*, 3853–3861. [CrossRef]
10. Nakagame, S.; Chandra, R.P.; Kadla, J.F.; Saddler, J.N. The isolation, characterization and effect of lignin isolated from steam pretreated Douglas-fir on the enzymatic hydrolysis of cellulose. *Bioresour Technol.* **2011**, *102*, 4507–4517. [CrossRef]
11. Luo, L.; Yuan, X.; Zhang, S.; Wang, X.; Li, M.; Wang, S. Effect of Pretreatments on the Enzymatic Hydrolysis of High-Yield Bamboo Chemo-Mechanical Pulp by Changing the Surface Lignin Content. *Polymers* **2021**, *13*, 787. [CrossRef]
12. Romero-Borbón, E.; Oropeza-González, A.E.; González-García, Y.; Córdova, J. Thermochemical and Enzymatic Saccharification of Water Hyacinth Biomass into Fermentable Sugars. *Processes* **2022**, *10*, 210. [CrossRef]
13. Meng, X.; Bhagia, S.; Wang, Y.; Zhou, Y.; Pu, Y.; Dunlap, J.R.; Shuai, L.; Ragauskas, A.J.; Yoo, C.G. Effects of the advanced organosolv pretreatment strategies on structural properties of woody biomass. *Ind. Crops Prod.* **2020**, *146*, 112144. [CrossRef]
14. Shi, F.; Xiang, H.; Li, Y. Combined pretreatment using ozonolysis and ball milling to improve enzymatic saccharification of corn straw. *Bioresour Technol.* **2015**, *179*, 444–451. [CrossRef]
15. Travaini, R.; Martin-Juarez, J.; Lorenzo-Hernando, A.; Bolado-Rodriguez, S. Ozonolysis: An advantageous pretreatment for lignocellulosic biomass revisited. *Bioresour Technol.* **2016**, *199*, 2–12. [CrossRef]
16. Garcia-Cubero, M.T.; Palacin, L.G.; Gonzalez-Benito, G.; Bolado, S.; Lucas, S.; Coca, M. An analysis of lignin removal in a fixed bed reactor by reaction of cereal straws with ozone. *Bioresour Technol.* **2012**, *107*, 229–234. [CrossRef]
17. Panneerselvam, A.; Sharma-Shivappa, R.R.; Kolar, P.; Clare, D.A.; Ranney, T. Hydrolysis of ozone pretreated energy grasses for optimal fermentable sugar production. *Bioresour Technol.* **2013**, *148*, 97–104. [CrossRef] [PubMed]
18. Perrone, O.M.; Rossi, J.S.; Moretti, M.M.S.; Nunes, C.; Bordignon, S.E.; Gomes, E.; Da-Silva, R.; Boscolo, M. Influence of ozonolysis time during sugarcane pretreatment: Effects on the fiber and enzymatic saccharification. *Bioresour Technol.* **2017**, *224*, 733–737. [CrossRef] [PubMed]
19. Travaini, R.; Otero, M.D.; Coca, M.; Da-Silva, R.; Bolado, S. Sugarcane bagasse ozonolysis pretreatment: Effect on enzymatic digestibility and inhibitory compound formation. *Bioresour Technol.* **2013**, *133*, 332–339. [CrossRef]
20. Andersen, S.L.F.; Castoldi, R.; Garcia, J.A.A.; Bracht, A.; Peralta, R.A.; de Lima, E.A.; Helm, C.V.; Moreira, R.D.F.P.M.; Peralta, R.M. Improving enzymatic saccharification of Eucalyptus grandis branches by ozone pretreatment. *Wood Sci. Technol.* **2018**, *53*, 49–69. [CrossRef]
21. Miura, T.; Lee, S.H.; Inoue, S.; Endo, T. Combined pretreatment using ozonolysis and wet-disk milling to improve enzymatic saccharification of Japanese cedar. *Bioresour Technol.* **2012**, *126*, 182–186. [CrossRef] [PubMed]
22. Yu, Z.; Jameel, H.; Chang, H.M.; Park, S. The effect of delignification of forest biomass on enzymatic hydrolysis. *Bioresour Technol.* **2011**, *102*, 9083–9089. [CrossRef] [PubMed]
23. Fang, S.; Wang, W.; Tong, S.; Zhang, C.; Liu, P. Evaluation of the Effects of Isolated Lignin on Cellulose Enzymatic Hydrolysis of Corn Stover Pretreatment by NaOH Combined with Ozone. *Molecules* **2018**, *23*, 1495. [CrossRef] [PubMed]
24. Wang, W.; Zhang, C.; Tong, S.; Cui, Z.; Liu, P. Enhanced Enzymatic Hydrolysis and Structural Features of Corn Stover by NaOH and Ozone Combined Pretreatment. *Molecules* **2018**, *23*, 1300. [CrossRef] [PubMed]
25. Osuna-Laveaga, D.R.; García-Depraect, O.; Vallejo-Rodríguez, R.; López-López, A.; León-Becerril, E. Integrated Ozonation-Enzymatic Hydrolysis Pretreatment of Sugarcane Bagasse: Enhancement of Sugars Released to Expended Ozone Ratio. *Processes* **2020**, *8*, 1274. [CrossRef]

26. Yao, L.; Yang, H.; Yoo, C.G.; Chen, C.; Meng, X.; Dai, J.; Yang, C.; Yu, J.; Ragauskas, A.J.; Chen, X. A mechanistic study of cellulase adsorption onto lignin. *Green Chem.* **2021**, *23*, 333–339. [CrossRef]
27. Szalaty, T.J.; Klapiszewski, L.; Stanisz, M.; Moszynski, D.; Skrzypczak, A.; Jesionowski, T. Catalyst-free activation of kraft lignin in air using hydrogen sulfate ionic liquids. *Int. J. Biol. Macromol.* **2018**, *119*, 431–437. [CrossRef] [PubMed]
28. Zhang, Y.; Wu, J.-Q.; Li, H.; Yuan, T.-Q.; Wang, Y.-Y.; Sun, R.-C. Heat Treatment of Industrial Alkaline Lignin and its Potential Application as an Adhesive for Green Wood–Lignin Composites. *ACS Sustain. Chem. Eng.* **2017**, *5*, 7269–7277. [CrossRef]
29. Yao, L.; Chen, C.; Yoo, C.G.; Meng, X.; Li, M.; Pu, Y.; Ragauskas, A.J.; Dong, C.; Yang, H. Insights of ethanol organosolv pretreatment on lignin properties of Broussonetia papyrifera. *ACS Sustain. Chem. Eng.* **2018**, *6*, 14767–14773. [CrossRef]
30. Yang, H.; Yoo, C.G.; Meng, X.; Pu, Y.; Muchero, W.; Tuskan, G.A.; Tschaplinski, T.J.; Ragauskas, A.J.; Yao, L. Structural changes of lignins in natural Populus variants during different pretreatments. *Bioresour Technol.* **2020**, *295*, 122240. [CrossRef] [PubMed]
31. Shi, C.; Zhang, S.; Wang, W.; Linhardt, R.J.; Ragauskas, A.J. Preparation of Highly Reactive Lignin by Ozone Oxidation: Application as Surfactants with Antioxidant and Anti-UV Properties. *ACS Sustain. Chem. Eng.* **2019**, *8*, 22–28. [CrossRef]
32. Wen, J.L.; Sun, S.L.; Yuan, T.Q.; Xu, F.; Sun, R.C. Structural elucidation of lignin polymers of Eucalyptus chips during organosolv pretreatment and extended delignification. *J. Agric. Food Chem.* **2013**, *61*, 11067–11075. [CrossRef] [PubMed]
33. Yao, L.; Yang, H.; Yoo, C.G.; Meng, X.; Pu, Y.; Hao, N.; Ragauskas, A.J. Characteristics of Lignin Fractions from Dilute Acid Pretreated Switchgrass and Their Effect on Cellobiohydrolase from Trichoderma longibrachiatum. *Front. Energy Res.* **2018**, *6*, 1. [CrossRef]
34. Sun, S.; Huang, Y.; Sun, R.; Tu, M. The strong association of condensed phenolic moieties in isolated lignins with their inhibition of enzymatic hydrolysis. *Green Chem.* **2016**, *18*, 4276–4286. [CrossRef]
35. Patri, A.S.; Mohan, R.; Pu, Y.; Yoo, C.G.; Ragauskas, A.J.; Kumar, R.; Kisailus, D.; Cai, C.M.; Wyman, C.E. THF co-solvent pretreatment prevents lignin redeposition from interfering with enzymes yielding prolonged cellulase activity. *Biotechnol. Biofuels* **2021**, *14*, 63. [CrossRef] [PubMed]
36. Yao, L.; Yang, H.; Yoo, C.G.; Meng, X.; Li, M.; Pu, Y.; Ragauskas, A.J.; Sykes, R.W. Adsorption of cellobiohydrolases I onto lignin fractions from dilute acid pretreated Broussonetia papyrifera. *Bioresour Technol.* **2017**, *244*, 957–962. [CrossRef]
37. Yang, H.; Jin, Y.; Shi, Z.; Wang, D.; Zhao, P.; Yang, J. Effect of hydrothermal pretreated bamboo lignin on cellulose saccharification for bioethanol production. *Ind. Crops Prod.* **2020**, *156*, 112865. [CrossRef]
38. Ying, W.; Shi, Z.; Yang, H.; Xu, G.; Zheng, Z.; Yang, J. Effect of alkaline lignin modification on cellulase-lignin interactions and enzymatic saccharification yield. *Biotechnol. Biofuels* **2018**, *11*, 214. [CrossRef]
39. Li, X.; Zheng, Y. Lignin-enzyme interaction: Mechanism, mitigation approach, modeling, and research prospects. *Biotechnol. Adv.* **2017**, *35*, 466–489. [CrossRef]
40. Wang, W.; Zhu, Y.; Du, J.; Yang, Y.; Jin, Y. Influence of lignin addition on the enzymatic digestibility of pretreated lignocellulosic biomasses. *Bioresour Technol.* **2015**, *181*, 7–12. [CrossRef]
41. Wu, K.; Shi, Z.; Yang, H.; Liao, Z.; Yang, J. Effect of ethanol organosolv lignin from bamboo on enzymatic hydrolysis of avicel. *ACS Sustain. Chem. Eng.* **2017**, *5*, 1721–1729. [CrossRef]
42. Nakagame, S.; Chandra, R.P.; Saddler, J.N. The effect of isolated lignins, obtained from a range of pretreated lignocellulosic substrates, on enzymatic hydrolysis. *Biotechnol. Bioeng.* **2010**, *105*, 871–879. [CrossRef] [PubMed]